Supplementary Information

Human neural cell type-specific extracellular vesicle proteome defines disease-related molecules associated with activated astrocytes in Alzheimer's disease brain

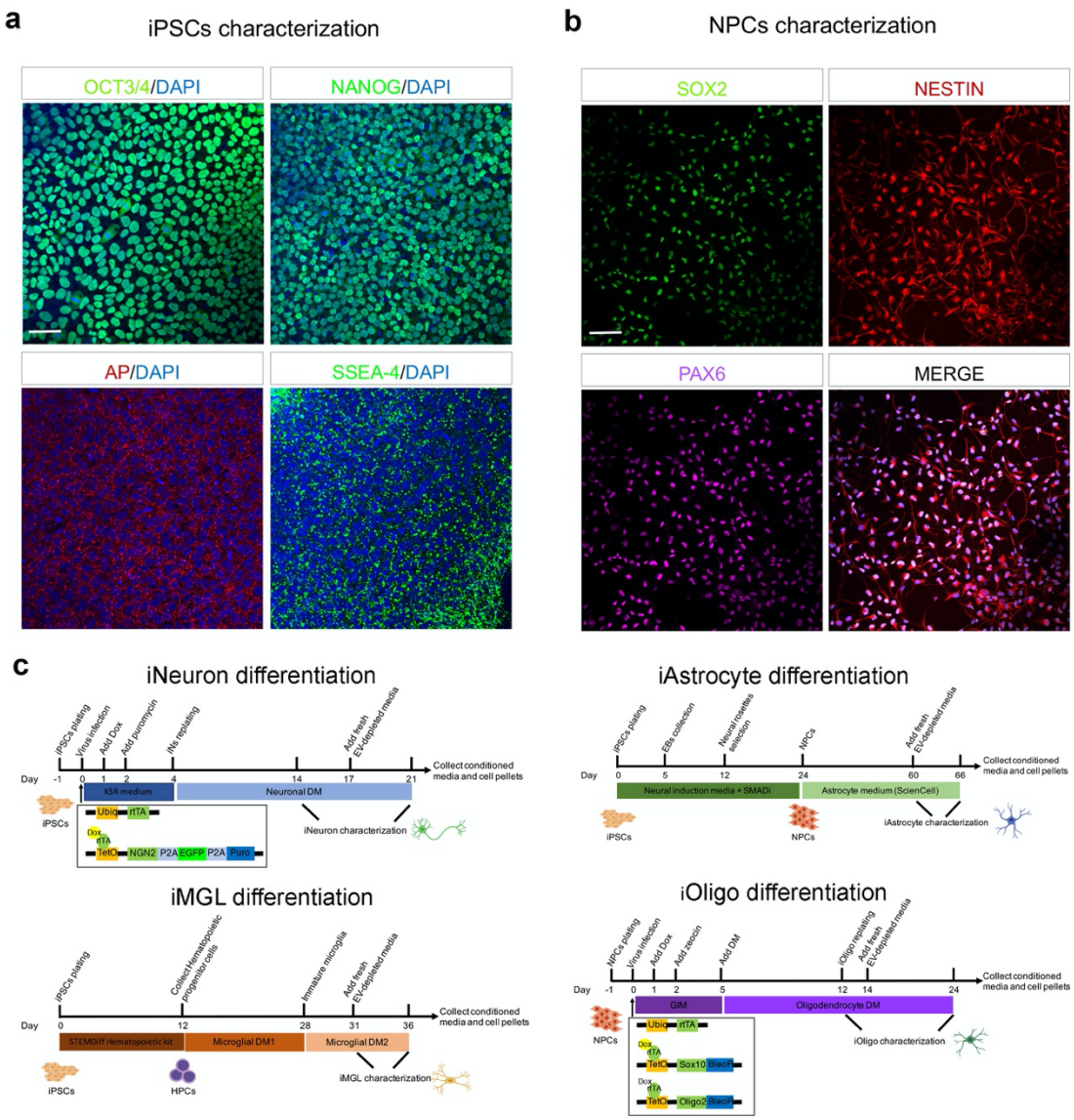

Supplementary Figure S1. Differentiation and characterization of human induced pluripotent stem cells and neural progenitor cells. a, Immuno-staining with pluripotent stem cell markers (OCT3/4, NANOG, AP and SSEA-4). Scale bar, 50 μm. **b**, Immuno-staining with neural progenitor cell markers (SOX2, NESTIN and PAX6). Scale bar, 75 μm. **c**, Schematic diagram of generating differentiated brain cells from induced pluripotent stem cells. iPSC, induced pluripotent stem cells; OCT3/4, octamer transcription factor-3/4; NANOG, homeobox protein NANOG; AP, alkaline phosphatase; SSEA-4, stage-specific embryonic antigen-4; SOX2, SRY-Box transcription factor 2; PAX6, paired Box 6; rtTA, reverse tetracycline-controlled transactivator; DM, differentiation media; NGN2, neurogenin-2; EB, embryonic body; NPC, neuronal progenitor cell; HPC, hematopoietic progenitor cell; Sox10, SRY-Box transcription factor 10; Olig2, oligodendrocyte transcription factor 2.

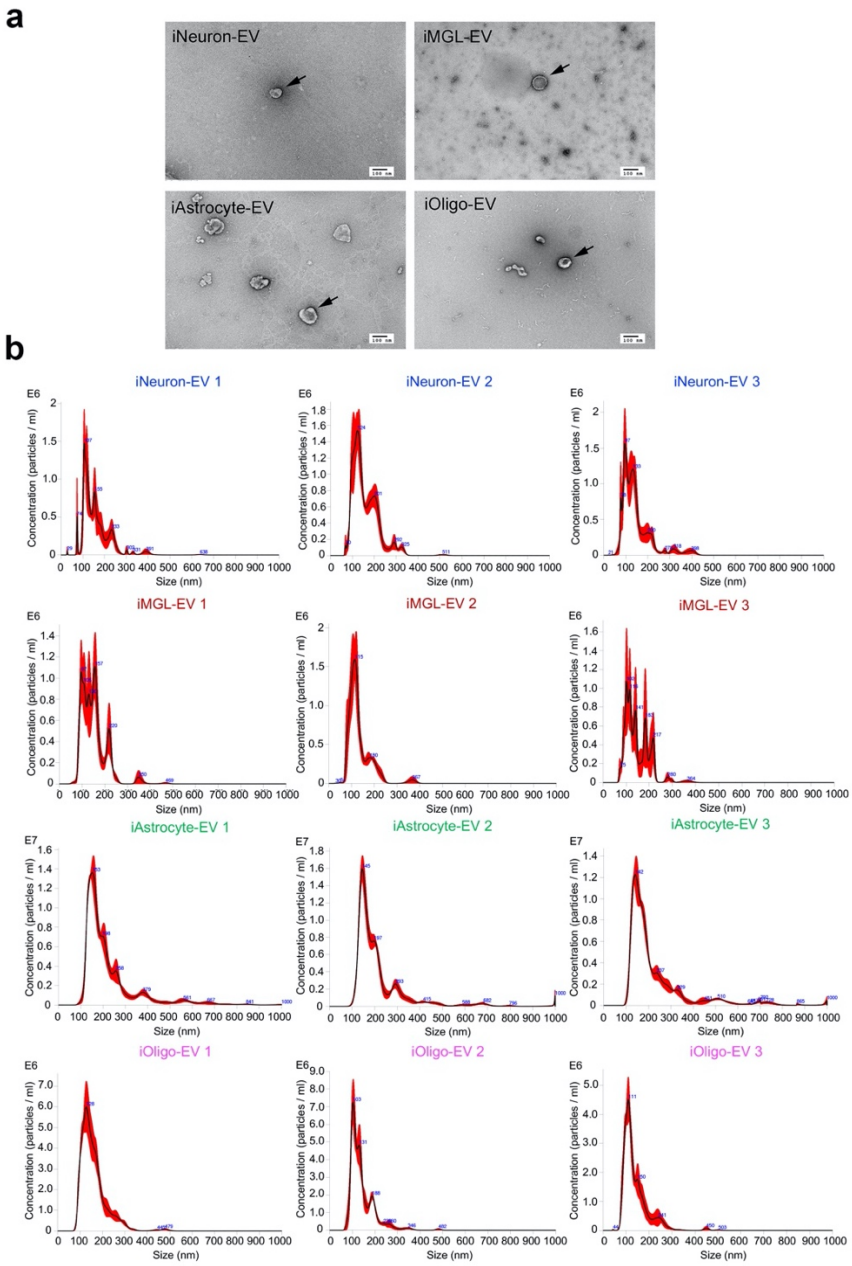

Supplementary Figure S2. Cell type specific EVs were examined by transmission electron microscopy and nanoparticle tracking analysis. a, The widefield transmission electron microscopy micrographs of isolated iNeuron-, iMGL-, iAstrocyte- and iOligo-EVs. The arrows indicated individual EVs shown in Figure 2a. Scale bar: 100 nm. **b**, EV size and number were determined by NTA. For each cell type, triplicates were tested. The black line shows the curve fitting; the red line represents the error of mean of the quadruplicate measurements. X axis indicates EV particle size (nm); Y axis indicates EV concentration (particles / ml). All the EV samples were pre-diluted with 1:10 in phosphate buffered saline before NTA examination. EV, extracellular vesicles; NTA, nanoparticle tracking analysis.

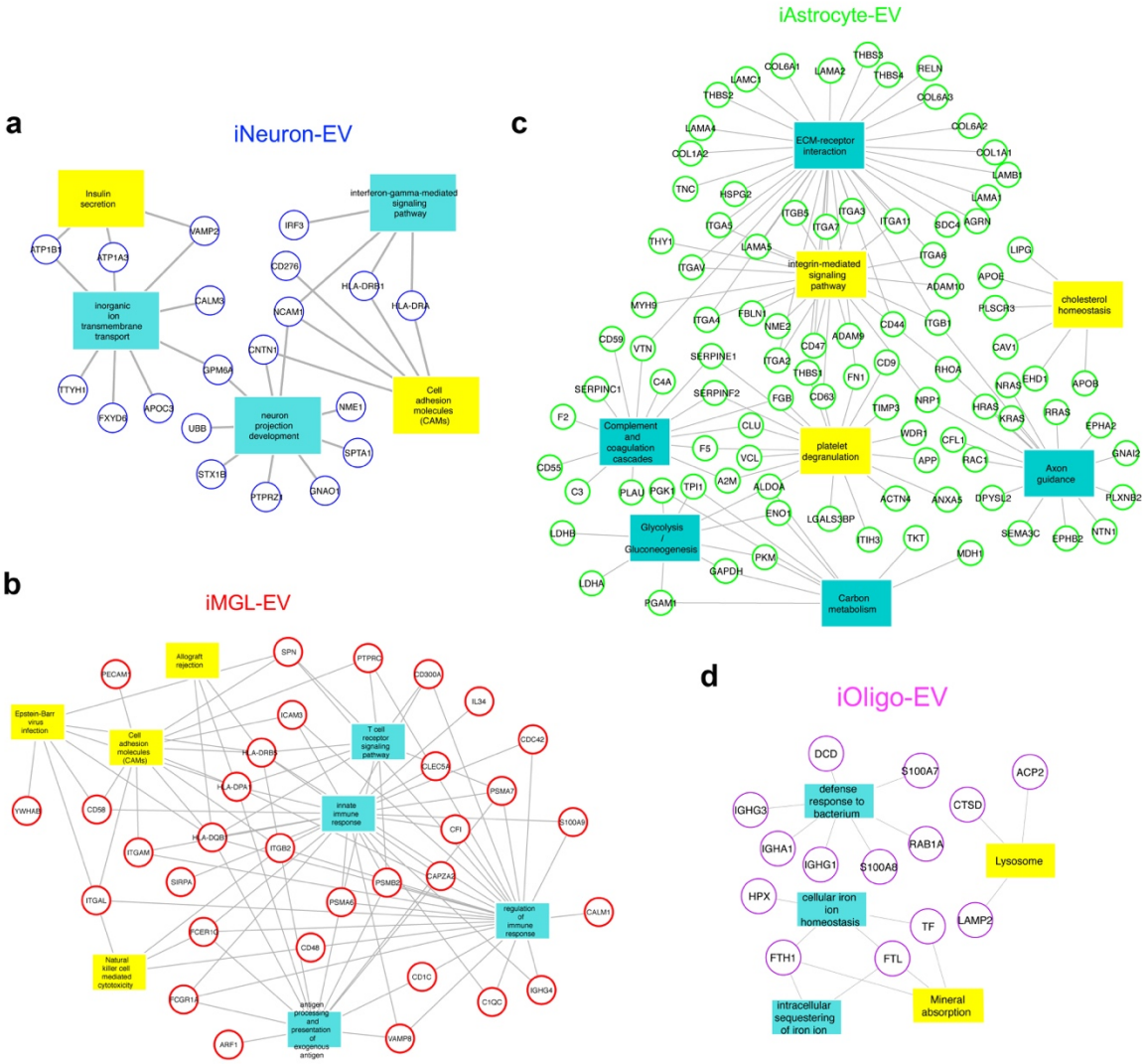

Supplementary Figure S3. Functional enrichment analysis of cell type specific EV signatures. Functional enrichment was conducted using the ToppCluster tool (FDR corrected, p-value < 0.05) (https://toppcluster.cchmc.org/) and Cytoscape v3.6.1. **a**, iNeuron-EV. **b**, iMGL-EV. **c**, iAstrocyte-EV. **d**, iOligo-EV. The yellow boxes indicate KEGG pathways; the light blue boxes indicated gene ontologies of biological processes. EV, extracellular vesicles; FDR, false discovery rate; KEGG, Kyoto encyclopedia of genes and genomes.

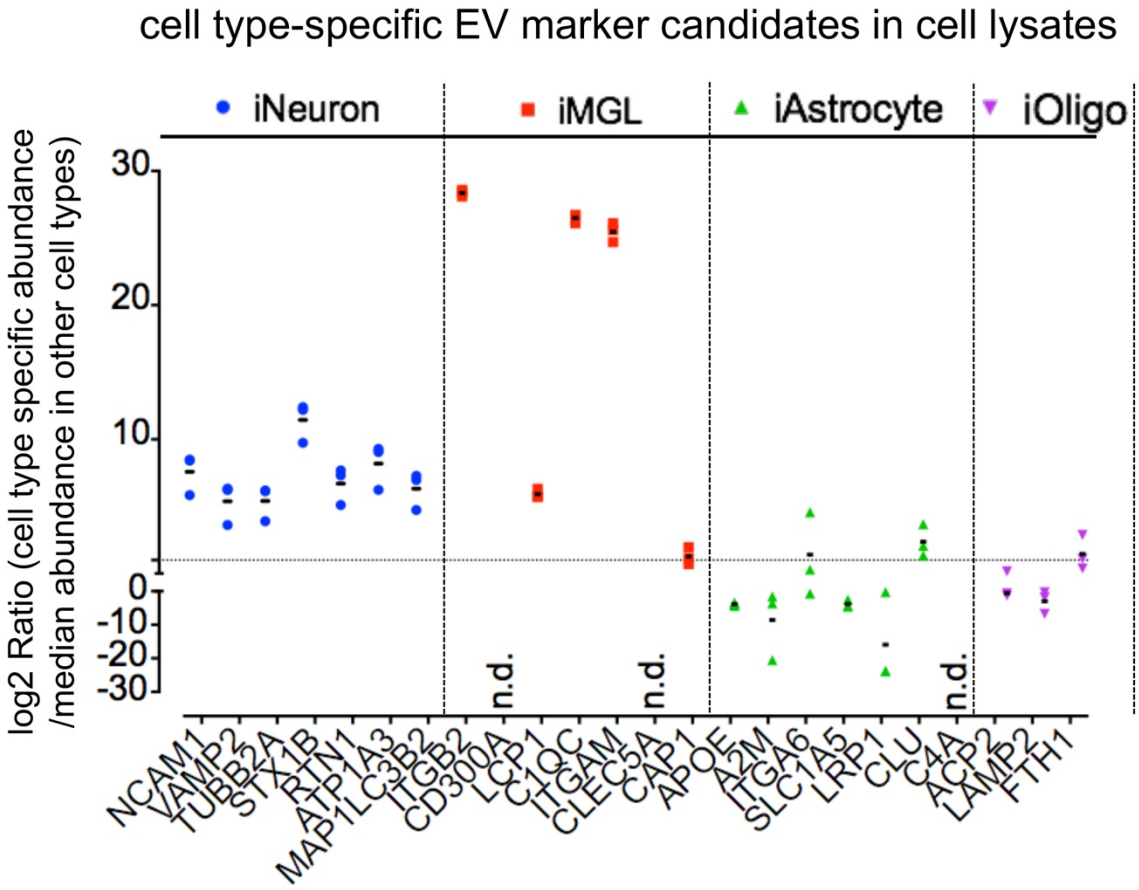

Supplementary Figure S4. Expression of selected cell type-specific EV marker candidates identified in their cellular origins. Log2 fold change of these selected marker candidates in individual replicates is shown in the specified cell type compared to other cell types. The dashed line indicated the value of y axis = 1 (fold change = 2). n.d., not determined. NCAM1; neural cell adhesion molecule 1, VAMP2, vesicle-associated membrane protein 2; TUBB2A, tubulin beta 2A class IIa; STX1B, syntaxin 1B; RTN1, reticulon-like protein 1; ATP1A3, ATPase Na+/K+ transporting subunit alpha 3; MAP1LC3B, microtubule-associated protein 1 light chain 3 beta; ITGB2, integrin beta 2; CD300A, CD300a molecule; LCP1, lymphocyte cytosolic protein 1; C1QC, complement C1q C chain; ITGAM, integrin M; CLEC5A, C-type lectin domain containing 5A; CAP1, cyclase associated actin cytoskeleton regulatory protein 1; APOE, apolipoprotein E; A2M, alpha-2 macroglobulin; ITGA6, integrin alpha 6; SLC1A5, solute carrier family 1 member 5; LRP1, low-density lipoprotein receptor-related protein 1; CLU, Clusterin/apolipoprotein J; C4A, complement C4A; ACP2, acid phosphatase 2; LAMP2, lysosomal associated membrane protein 2; FTH1, ferritin heavy chain 1.

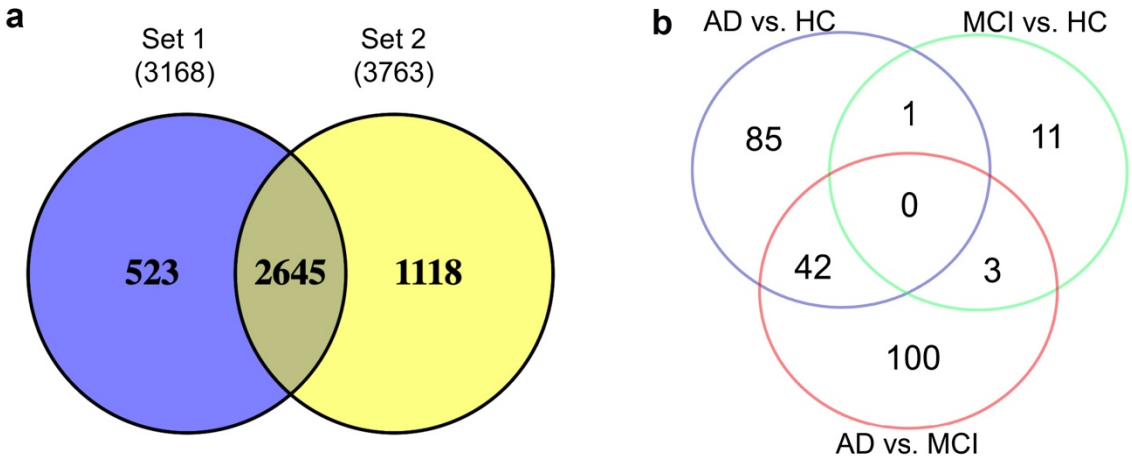

Supplementary Figure S5. Differential abundance of EV proteins identified in HC, MCI and AD brain by 16-plex TMT-labeled mass spectrometry. **a**, Venn diagram showing a total of 3168 proteins identified in set 1 of the TMT-labeled mass spectrometry and 3763 proteins in set 2 of the TMT-labeled mass spectrometry. The overlapped 2645 proteins were then selected for human brain-derived EV proteomic analysis. **b**, Venn diagram showing a total of 242 brain-derived EV proteins that were determined to be significantly altered (decreased or increased) by ANOVA ($p < 0.05$) followed by Tukey's post hoc test ($p < 0.01$) among the three groups by comparisons with (1) AD versus HC, (2) MCI versus HC, and (3) AD versus MCI. EV, extracellular vesicles; HC, healthy control; MCI, mild cognitive impairment; AD, Alzheimer's disease; TMT, tandem mass tag; ANOVA, analysis of variances.

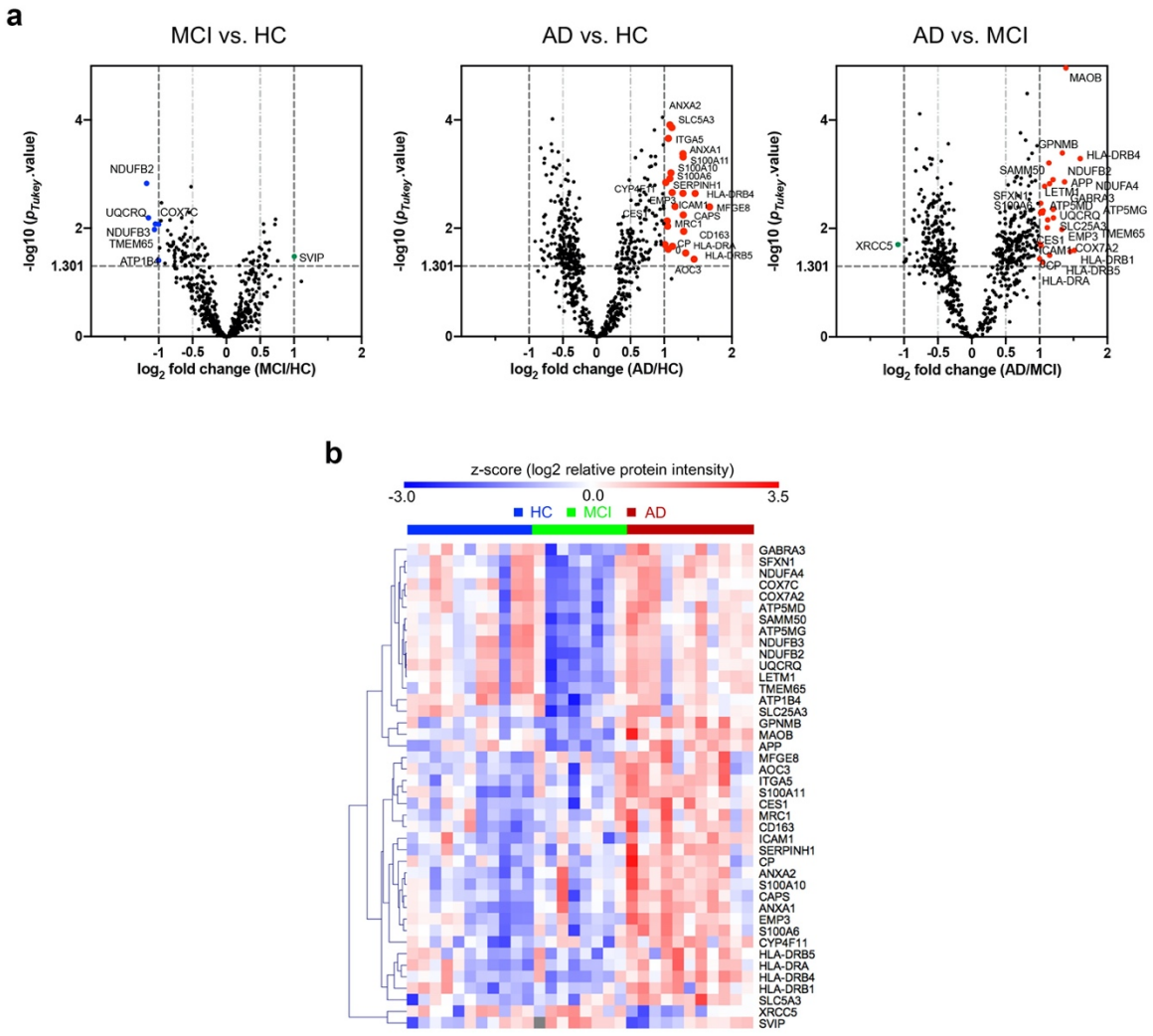

Supplementary Figure S6. Significantly differentially expressed proteins in EVs among the three groups. a, Volcano plot representing a degree of differential expression of EV proteins in HC, MCI, and AD. MCI vs. HC (Left panel), AD vs. HC (middle panel), AD vs. MCI (right panel). X-axis indicates log transformed fold change in expression; Y-axis indicates log-transformed post hoc Tukey's test. Grey dashed lines indicate the cutoff of p value = 0.05, and log2 fold change =1 or -1; Light grey dashed lines indicate the cutoff of log2 fold change =0.5 or -0.5. **b**, Heatmap of z-scored log2 relative protein intensity within each EV sample after unsupervised hierarchical clustering showing the significantly differentially expressed proteins (sDEPs) in the three comparisons (HC versus AD, HC versus MCI, MCI versus AD) determined by Tukey's post hoc test $p < 0.05$ and fold change > 2 (log2 FC > 1 or < -1). EV, extracellular vesicles; HC, healthy control; MCI, mild cognitive impairment; AD, Alzheimer's disease; TMT, tandem mass tag; sDEPs, significantly differentially expressed proteins.

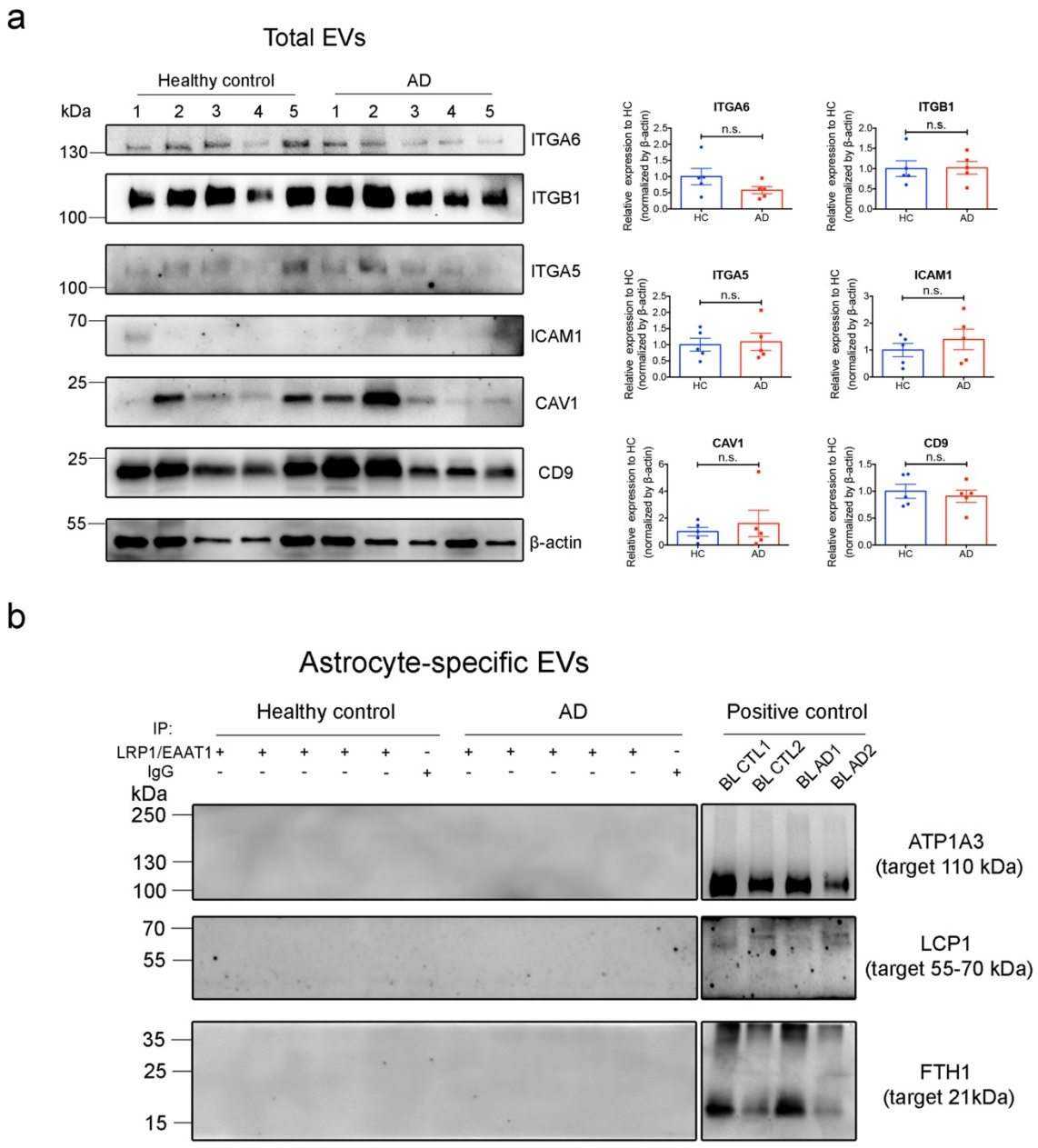

Supplementary Figure S7. Western blot analysis of selected M7 module members in total brain-derived EVs and astrocyte-specific EVs isolated from HC and AD patients. a, No selected protein levels were found significantly changed in total EVs from AD (n = 5) compared to HC samples (n = 5). The western blot signals were calculated using ImageJ and normalized by β-actin intensity. Data are presented as mean ± SEM, n.s., no significance, using Mann-Whitney non-parametric test. **b,** Western blot analysis of some other cell-type specific EV proteins in astrocyte-specific EVs immunoprecipitated from HC and AD patients, as well as positive control samples from brain lysates of HC and AD patients. The potential neuron-specific EV protein ATP1A3, microglia-specific EV protein LCP1, and oligodendrocyte-specific EV protein FTH1 was shown in positive controls, but undetectable in astrocyte-specific EVs. The original western blot images were shown in Supplementary Fig. 9. EVs, extracellular vesicles; BL, brain lysate; AD, Alzheimer's disease.

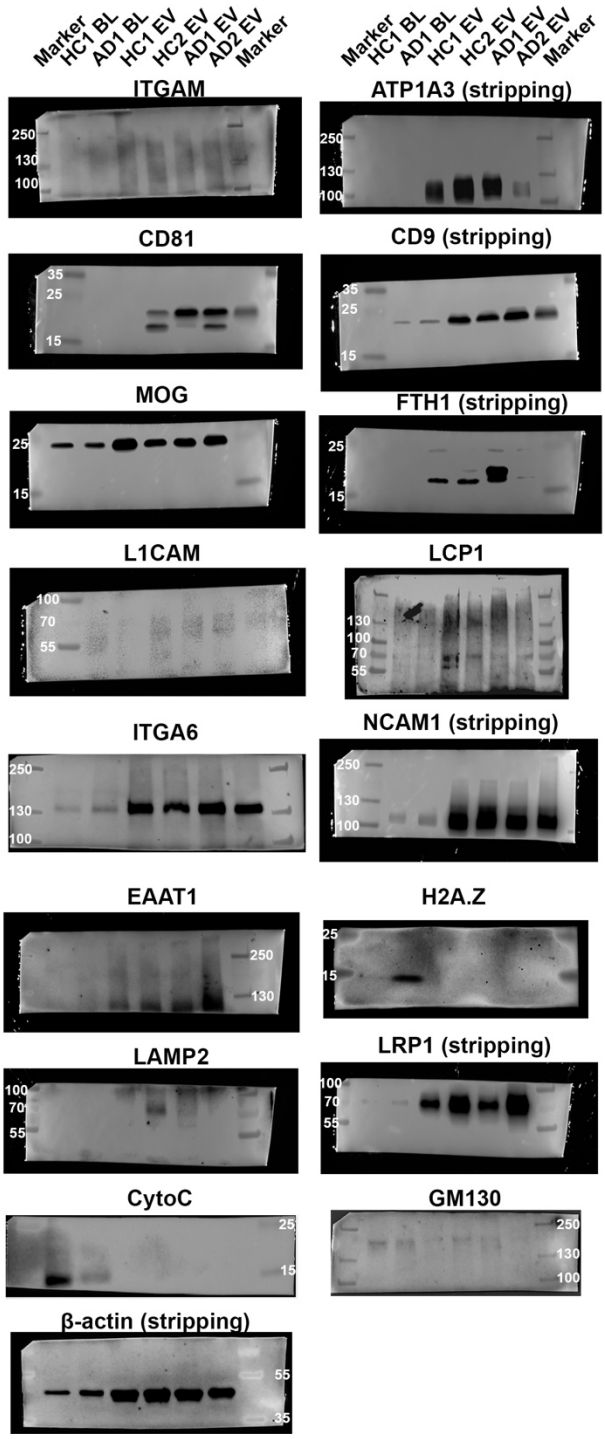

Supplementary Figure S8. Original western blot images of brain lysates and associated EVs isolated from both HC and AD patients (attached to Fig. 4d). Stripping indicates that the protein was detected after original membrane stripping.

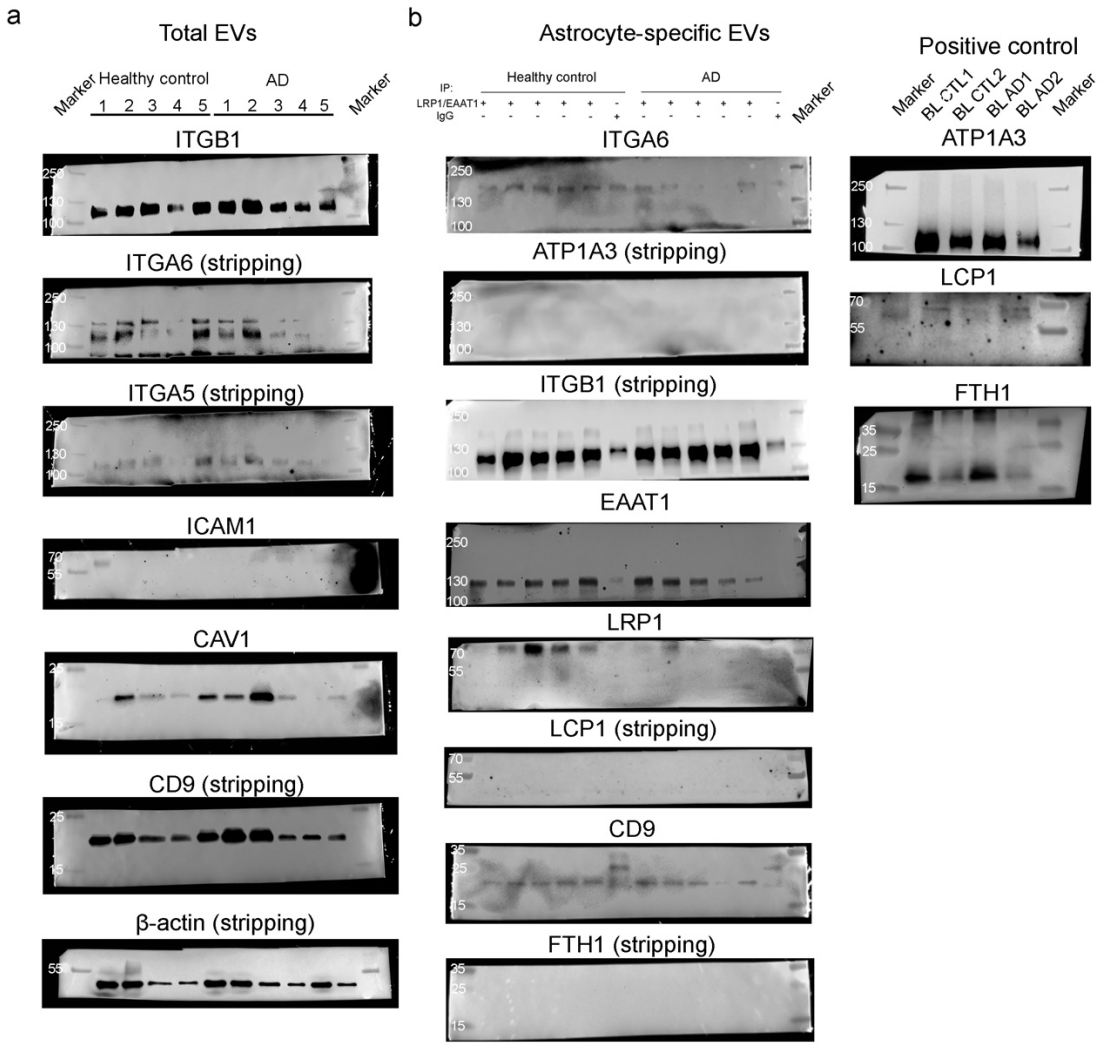

Supplementary Figure S9. Original western blot images of selected M7 module members in total brain-derived EVs and astrocyte-specific EVs isolated from HC and AD patients. a, Original western blot images for total brain-derived EVs attached to Supplementary Fig. 7a. **b,** Original western blot images for astrocyte-specific EVs attached to Fig. 7f and Supplementary Fig. 7b. Stripping indicates that the protein was detected after original membrane stripping.